Geomechanics and Engineering, *Vol. 24, No. 6 (2021) 589-597*
DOI: https://doi.org/10.12989/gae.2021.24.6.589

Numerical investigation of geocell reinforced slopes behavior by considering geocell geometry effect

Alireza Ardakani* and Ali Namaei

Department of Civil Engineering, Imam Khomeini International University, Qazvin, Iran

(Received January 30, 2021, Revised March 12, 2021, Accepted March 18, 2021)

Abstract. The present study evaluates geocell reinforced slope behavior. A three dimensional analysis is carried out to simulate soil and geocell elastoplastic behavior using the finite difference software FLAC^{3D}. In order to investigate the geocell reinforcement effect, the geocell aperture size, thickness, geocell placement condition and soil compaction had been considered as variable parameters. Moreover, a comparison is evaluated between geocell reinforcing system and conventional planar reinforcement. The obtained results showed that the pocket size, thickness and soil compaction have considerable influence on the geocell reinforcement slope performance. Moreover, it was found that the critical sliding surface was bounded by the first geocell reinforcement and the slope stability increases, by increasing the vertical space between geocell layers. In addition, the comparison between geocell and geogrid reinforcement indicates the efficiency of using cellular honeycomb geosynthetic reinforcement.

Keywords: geocell; slope stability; three dimensional; aperture size; safety factor

1. Introduction

Geosynthetics is a highly attractive element for stabilizing embankment, rail track, slopes, foundation and retaining wall due to their economic consideration which it offers in comparison with conventional retaining systems (Guerrero and Vallejo 2010, Guo *et al*. 2014, Won *et al*. 2016, Jesmani *et al*. 2016, Moltagh *et al*. 2018, Halder and Chakraborty 2020, Garcia and Neto 2021). Geocell mattresses are one type of three dimensional and honeycomb soil reinforcements which manufactured from polyethylene sheets using ultrasonically welded joints. This system can effectively confine the infilled soil by the sheets which make it suitable for soil reinforcement (Dash *et al*. 2003, Latha *et al*. 2008).

Several studies have been carried out, in order to assess the behavior of geocell reinforced foundations (Dash *et al*. 2001, Latha and Somwanshi 2009, Saride *et al*. 2013, Tafreshi *et al*. 2015, Khalaj *et al*. 2015, Biswas and Mittal 2017). For instance, Zhao *et al*. (2009) investigated the behavior of embankments overlaying on geocell reinforced layers. They divided the geocell mattress functions in three aspects: (a) Lateral resistance effect; (b) vertical stress dispersion effect; and (c) membrane effect. Also, Dash (2010) showed that the geocell reinforced layer behaves as a wide slab. The geocell mattress transmits the applied surcharge pressure to the beneath soil layers over a wider width. Moreover, to protect buried pipes, Tavakoli *et al*. (2013) utilized geocell for trench reinforcement. In this study, further assessment of the geocell behavior with varied opening areas and heights, positioning over the buried structures under repeated loads have been investigated. It was found that installation of the geocell in the backfill with specific compaction increases the backfill bearing capacity. Hedge and Sitharam (2016) used geocell to improve the soft clay foundation bearing capacity under incremental cyclic loading. They showed that geocell layer increase the elastic deformation of clayey bed. Moreover, the presence of geocell layer has a significant effect on the foundation natural frequency and the amplitude of vibration. Oliaei and Kouzegaran (2017) evaluated the efficiency of geocell for foundation reinforcement numerically in both sandy and clayey beds. The results indicated by increasing the bearing capacity and decreasing the settlements the geocells in both sandy and clayey soil improvement are significantly more efficient than planar geosynthetics. Recently, it has been seen that geocell usages have been increased in other geotechnical problems such as soil improvement against liquefaction (Kumar *et al*. 2019).

In contrast with the considerable studies on geocell reinforcing foundations, limited investigations have been conducted to assess the geocell reinforced retaining walls or slopes behavior. Latha and Rajagopal (2007) used an equivalent two dimensional model to evaluate the effect of geocell in embankments reinforcing. They found that the geocell was preserved as an equivalent soil layer with cohesive strength and stiffness due to the geocell. Chen and Chiu (2008) simulated a geocell reinforced retaining wall. They showed that the maximum lateral displacement decreases and occurred at the mid-height of the wall by placing geocell upper. On the other hand, the maximum lateral deflection increased by placing the geocell mattress in the lower part of the wall. Ling *et al*. (2009) examined the slope geocell reinforced behavior under seismic conditions and recommended the equivalent pseudo static

*Corresponding author, Associate Professor
E-mail: a.ardakani@eng.ikiu.ac.ir

ISSN: 2005-307X (Print), 2092-6219 (Online)

coefficients for analyzing earthquake resistance geocell retaining walls. Chen *et al*. (2013) investigated the effective parameter on the geocell reinforced retaining wall. Their results showed that a wall with a facing angle less than 80% will significantly reduce the lateral displacement of the wall face. Mehdipour *et al*. (2013, 2017) assessed the stability of geocell reinforced slopes using equivalent two dimensional analyses. The results indicate that the reinforcing mechanism of geocell reinforcement is considerably related to the geocell thickness. The mobilized flexural strength and vertical frictional resistance magnify as the height of the geocell increases. Compared with planar reinforcement, a smaller quantity of geocell reinforcement is required to achieve an equivalent factor of safety value. Song *et al*. (2017) evaluated the stability of geocell reinforced wall. They used limit equilibrium method to predict the global stability of the reinforced wall. They showed that classical theories of earth pressure are not suitable for analyzing the stability of geocell reinforced walls. Also, Song *et al*. (2018) assessed the failure modes of geocell reinforced retaining wall. The study results indicated when the apparent cohesion was very large, or the friction between the wall and the footing was small or there existed a weak interlayer in the wall, sliding failure was found to occur in geocell reinforced retaining walls, similar to the failure mode of rigid retaining walls. Dai *et al*. (2018) used a series of model tests to investigate the performance of embankment geocell reinforced under static and cyclic loading. They concluded that shallower the geocell layer was embedded, the better stability of the embankment was. Arvin *et al*. (2019) and Kazemian and Arvin (2019) used three dimensional strength reduction analyses to assess the behavior of geocell reinforced slope safety factor. They showed that the geocell layer forms a stiff layer which increases the slope safety factor by inducing a more uniform stress distribution. Song and Tian (2019) recommended a new three dimensional numerical approach to simulate geocell reinforced foundation soils that the geocell was modeled as membrane elements and the complex interaction between geocell and soil was recognized by coupling their degrees of freedom. Their results indicated that the decrease in geocell pocket size has a significant effect on the bearing capacity increase. Also, it was found that the geocell thickness showed an insignificant influence on the bearing capacity when the pocket size kept constant. Moreover, comparison with field data illustrated that this simulation method could efficiently predicted the behavior of geocell.

In the aforementioned investigations, the beneficial effect of geocell reinforcement in slopes and retaining walls stabilization has been discussed. As there are very few available design methods for geocell reinforcement slope and embankment. One traditional method is slip line, the other is equivalent two dimensional method, and also a method based on slope stability or a deformation based method such as considering geocell as a Winkler beam (Latha 2011, Zhao and Zhao 2013). Still, no comprehensive design and test methods have been available to incorporate all the effective factors for geocell reinforcement retaining walls and slopes. Therefore, more research is desired for developing reliable design and test methods for geocell usages in slope stability.

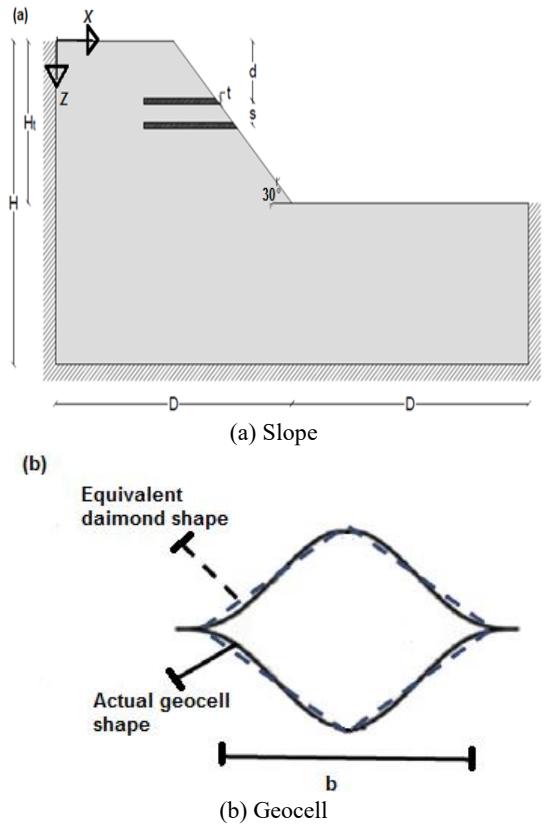

(a) Slope

(b) Geocell

Fig. 1 A schematic view of the model used in this evaluation

As numerical approaches can predict most of the geotechnical problems (Ardakani *et al*. 2014, Bayat *et al*. 2016, 2018), in this research, several influential factors were evaluated based on numerical three dimensional geocell reinforced slope analysis. Some factors have not been well investigated before, such as the effects of aperture size, thickness, soil compaction, effective geocell placement and vertical spacing between geocell layers. The displacements and the safety factor of slope are measured and discussed in detail. Also, the mobilized stresses were assessed in order to examine the degree of passive resistance and lateral pressure over the geocell strip in the reinforced slopes. In addition, the real geocell tensile behavior were considered and applied with fish function.

2. Numerical analysis

In this study, the behavior of the geocell reinforced slope is investigated by using the finite difference method. A schematic view of the slope and equivalent diamond geocell simulated in this evaluation is illustrated in Fig. 1 in which S is the vertical geocell layers spacing, L is length of geocell layers, t indicates the geocell height and D and H are the distances from the slope foundation to the bottom and on the side boundaries of the modeled zone, respectively.

The soil used for analysis was sub-angular silica sand

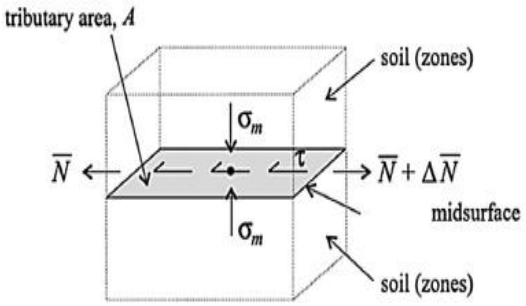

Fig. 2 Stresses induced on the geogrid elements (Itasca 2005)

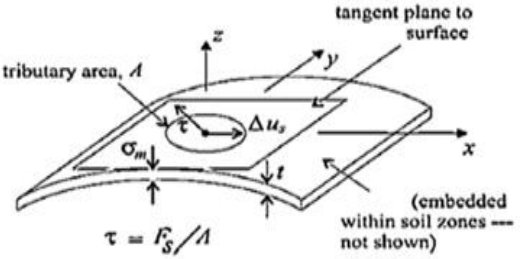

(a) Shear stress acting at each node

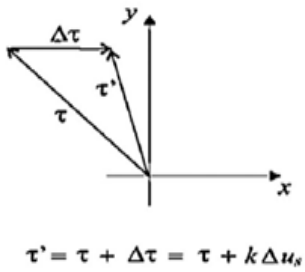

(b) Shear stress at each time step

Fig. 3 Interface behavior at a geogrid node (Itcasa 2005)

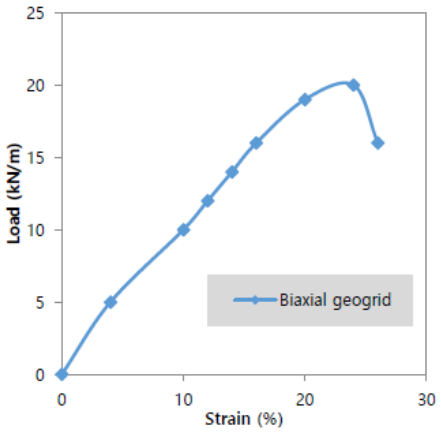

Fig. 4 Load-strain behavior of BX geogrid (Dash 2012)

and three sets of 50, 60, 70% relative densities. The soil was classified as SP according to the Unified Soil Classification System (USCS). Furthermore, Chen *et al*. (2013) conducted triaxial test on this sand samples with various relative densities showed that the Young's modulus and peak friction angle of this sand increased with relative density and reduced as the confining pressure increased. Chen *et al*.

Table 1 Properties of soil and geocell used in numerical analysis

Soil properties	
Cohesion (kPa)	0
Poisson's ratio	0.3
Maximum unit weight (kN/m^3)	13.8
Minimum unit weight (kN/m^3)	16.6
Relative density (%)	50, 60, 70
Geocell properties	
Tensile yield strength (kN/m)	60
Secant modulus at stain 10 % (kN/m)	125
Height (mm)	100, 150, 200, 250, 300
Aperture size (cm × cm)	15 × 15, 25 × 25, 35 × 35

(2013) represented Eqs. (1) and (2) for calculating the peak friction angle and Young's modulus, respectively. Also, relative density computed from Eq. (3). In these equations D_r, P_a and σ_3 are relative density, atmospheric pressure and confining pressure, respectively. The Mohr-Coulomb model is used for representing shear failure in soil. The geocell used in this study is manufactured from biaxial geogrid (BX) used by Krishnaswamy *et al*. (2000). The geocell layer is modeled as an equivalent diamond using geogrid elements in FLAC. Geogrid structural elements are three-noded, flat, finite elements that are assigned a finite-element type that resists membrane but does not resist bending loading. In this study, geogrid elements behave as an isotropic, linearly elastic material with no failure limit. The stresses on the geogrid element are shown in Fig. 2. The membrane stresses which develop in the geogrid balanced the effective confining stress σ_m and total shear stress τ. The interaction of geogrid with surrounding soil is calculated at each element node by a rigid attachment in the normal direction and a friction cohesion behavior in the tangent plane to the geogrid element surface. Interface behavior at a geogrid node is shown in Fig. 3 (Itasca 2005). Also, the geocell layers were set free to deform in all direction in order to consider the real behavior of geocells.

$$\varphi = 30.8 + 13.4\ D_r - 4.2 D_r \log\left(\frac{\sigma_3}{P_a}\right) \quad (1)$$

$$E = (290 + 177 D_r) P_a \left(\frac{\sigma_3}{P_a}\right)^{0.55} \quad (2)$$

$$D_r = \frac{\gamma_d - \gamma_{min}}{\gamma_{max} - \gamma_{min}} \frac{\gamma_{max}}{\gamma_d} \quad (3)$$

As the behavior of geocells changes from elastic to elastic-plastic one, a FISH code is carried out to apply this behavior on the simulated geocells in order to reach more practical results. The load-strain behavior of used geocells has been investigated by Krishnaswamy *et al*. (2000). This load-strain behavior is illustrated in Fig. 4. The geogrid-soil interaction is cohesive and frictional. In this model, Mohr-Coulomb failure model was used to simulate the interaction between the geocell and the surrounding soil. In this assessment, the geocell-soil interface coefficient is set as

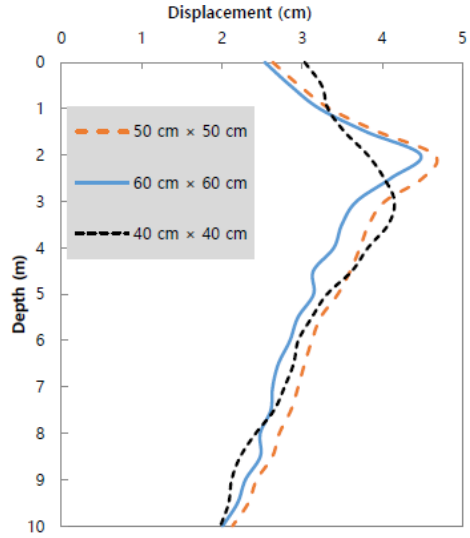

Fig. 5 Sensitivity analysis on mesh dimensions on slope displacement

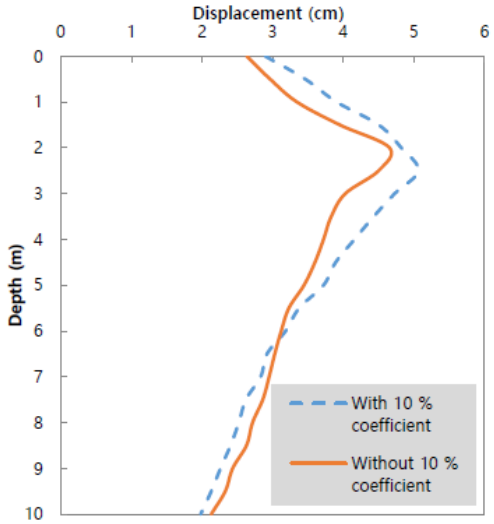

Fig. 6 The effect of mesh incremental coefficient on slope displacement

2/3 in order to consider the effect of side interaction occurred between geocell pockets and filled martials as a result of vertical loading. This value is chosen, as a common value suggested by Leshchinsky and Ling (2013) The input parameters for the geogrid elements are geogrid thickness, tensile yield strength, Poisson's ratio and Young's modulus. The properties of soil, geocells and the properties of geogrid used to compare between the behavior of geocell and geogrid, are presented in Table 1.

In order to assess the mesh dimensions effect on the numerical modeling results, a series of sensitivity analyses were conducted with 0.6 m × 0.6 m, 0.5 m × 0.5 m and 0.4 m × 0.4 m mesh dimension in *x*-*z* plane with constant 1 m mesh dimension along *y* direction. The 25 cm × 25 cm geocell aperture size with 10 m length in 60% relative density of sand was used for this sensitivity analysis. The horizontal displacements from the top of the slope have been considered as the results of the mesh this analysis and

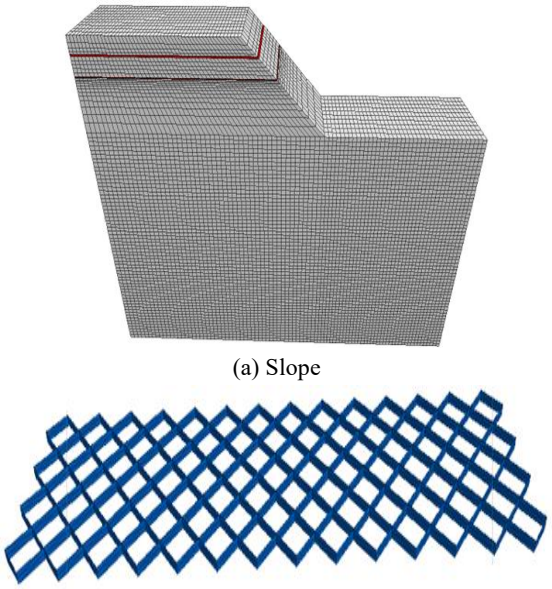

(a) Slope

(b) Geocell

Fig. 7 The final model meshing and boundaries configuration

illustrated in Fig. 5. It is indicating that decreasing zones size lower than 0.5 m × 0.5 m, the mesh sizes along *x*-*z* plane have no more influence on the analyses results.

In order to reduce the analysis time without changing the results, the mesh dimension along *z*-axis was fixed to increase 10% from the geocell layers with respect to those in the prior zone. Several factors have contributed to the 10% chosen. For instance, the mesh dimensions should be fine and the ratio of the longest edge to the shortest edge should be close to one where the stress concentration or rapid strain changes occur, but using unsuitable zones in the boundary areas causes no major error in the results (Ou 2006).

A series of analysis was conducted to investigate the accuracy of the modeling result with 10% mesh dimension increase along *z*-axis. The results of applying the mesh-size coefficient are given in Fig. 6. As can be seen from this figure, applying the mesh-size coefficient to the meshing does not have a significant influence on the slope behavior.

For evaluating the boundary effect from the slope crest, three different distances 40, 50 and 60 m from the slope crest to the model boundary were considered. The results indicated that by taking 50 m the boundary distance from the slope crest, the analysis results showed a satisfactory level of error. The fixity of *x* and *y* directions boundaries were along to *x* and *y*, respectively. Also, the bedrock was assumed to be in 40 m depth from top of the slope. The final meshing and boundaries configuration is illustrated in Fig. 7.

3. Verification

The verification of the numerical analysis is validated by comparing the results with a model test available report. Krishnaswamy *et al*. (2000) conducted a series of model

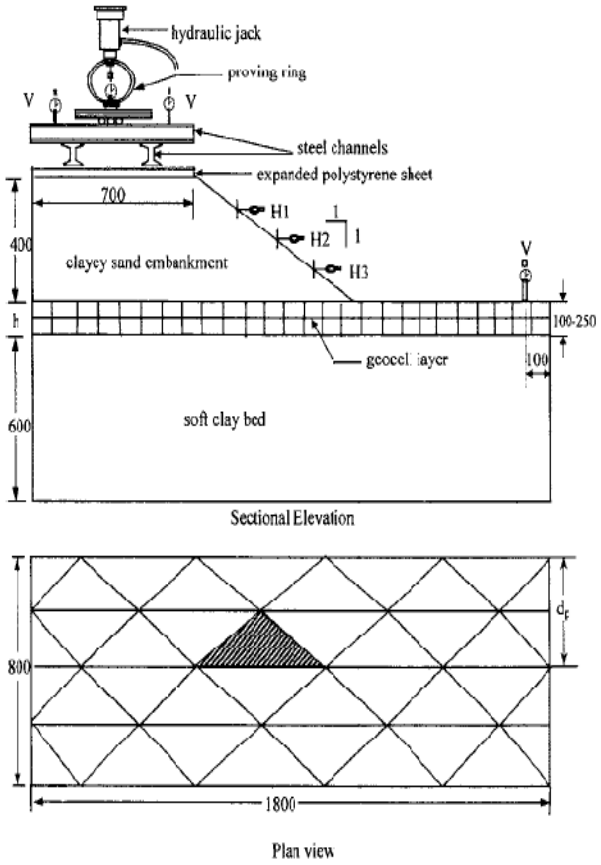

Fig. 8 The embankment constructed by Krishnaswamy *et al*. (2000)

Table 2 Properties of soils and geocell used for verification

Soft clay properties	
Friction angle (Degree)	0
Cohesion (kPa)	10
Unit weight (kN/m^3)	17
Young's modulus (MPa)	200
Clayey sand properties	
Friction angle (Degree)	30
Cohesion (kPa)	10
Unit weight (kN/m^3)	19
Young's modulus (MPa)	380
BX geocell properties	
Secant modulus at 10% strain level (kN/m)	125
Secant modulus at 5% strain level (kN/m)	160
Thickness (mm)	100
Ultimate tensile strength (kN/m)	20

tests on diamond pattern BX geocell reinforced embankments. The embankment was placed on a layer of geocell which used to reinforce the soft clay subgrade. Above the geocell layer, the embankment was constructed using clayey sand. The constructed embankment chosen for verification is illustrated in Fig. 8, and the properties of soft clay, clayey sand and BX geocell are given in Table 2. In

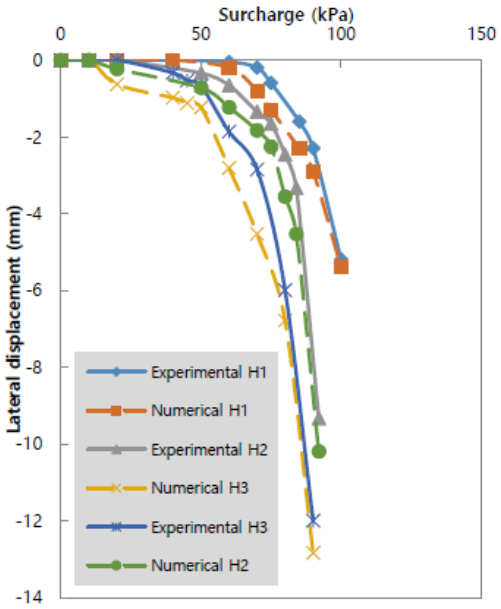

Fig. 9 Comparison between the obtained results and model tests of Krishnaswamy *et al*. (2000)

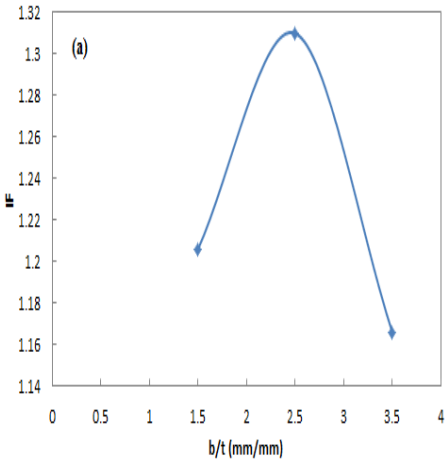

(a) Safety factor

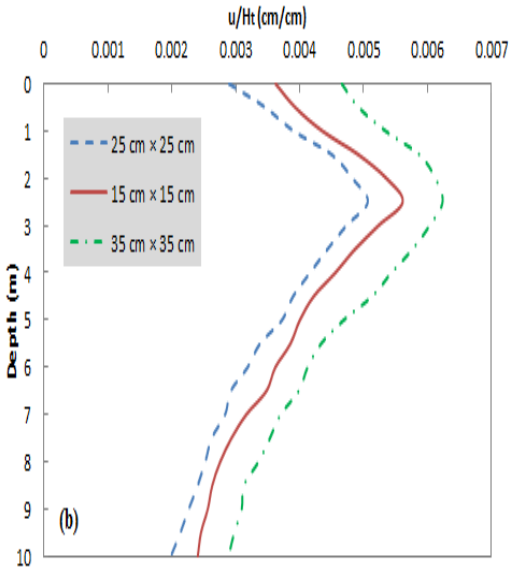

(b) Slope displacement

Fig. 10 Effect of geocell aperture size on (a) and (b)

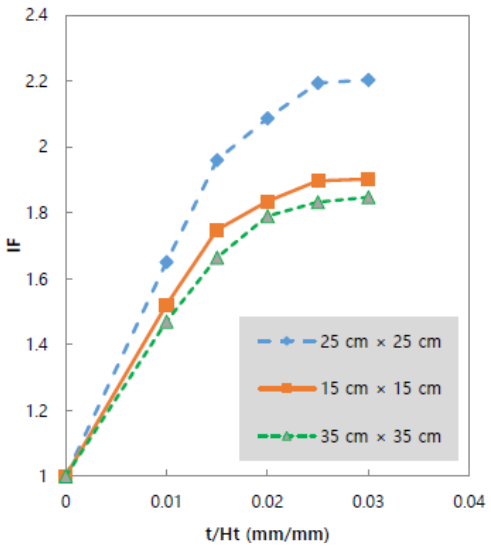

Fig. 11 Effect of geocell thickness on safety factor

Table 3 Effect of soil relative density on geocell reinforced slope behavior

Soil relative density (%)	50	60	70
IF	1.18	1.31	1.45
$u_{max}\,(cm)$	7	5	4
Maximum membrane stress (kPa)	0.03	0.04	0.05

this Table, as the secant modulus varies with tensile strain level and it cannot be considered in this finite difference method, the secant modulus of geocell conservatively is set 125 kN/m occurred in 10% strain level.

Fig. 9 illustrates the comparison between results of the 3D analysis and the experimental model test for H1, H2 and H3 LVDT presented by Krishnaswamy *et al*. (2000). It is generally found that the experimental tests conducted by Krishnaswamy *et al*. (2000) have good agreement with the current numerical study which shows that the present numerical modeling is verified. Also, the higher lateral displacement at higher surcharge pressure in numerical analysis is seen. This is due to the difference between the three dimensional numerical analysis and the small scale experimental one.

4. Results and discussion

In this section the effects of aperture size, thickness, soil compaction, suitable geocell layer placement in the slope depth and vertical spacing between geocell layers is evaluated. In order to investigate these parameters effect, a series of slope stability analyses have been conducted. The safety factor of geocell reinforced slopes is defined with a non-dimensional value called improvement factor calculated as Eq. (4), wherein $SF_{reinforced}$ and $SF_{unreinforced}$ are the safety factor of reinforced and unreinforced slopes, respectively. In addition, a stress investigation of geocell layers is presented and the mobilized passive resistance is discussed. Furthermore, a comparison has been evaluated between the geocell and planar geosynthetics slope stabilization.

$$IF = \frac{SF_{reinforced}}{SF_{unreinforced}} \tag{4}$$

Fig. 10 illustrates the effect of geocell aperture size on IF and lateral displacement of slope, respectively. In the figures, u represents the lateral displacement and b represents biggest dimension of geocell pocket size which are non-dimensioned versus slope height (H_t) and geocell thickness (t), respectively. Also, the amounts of IF and displacement are presented for constant relative density (60%), thickness (100 mm), vertical spacing (2 m) and depth of first layer (2 m) in order to attain meaningful data.

Fig. 10(a) shows variation of IF versus geocell aperture size and Fig. 10(b) shows the slope displacement for different geocell aperture size. The assessment of these two figures shows that IF and lateral displacement increase by increasing the geocell pocket size, although the rate of slope stability improvement has been decreased for higher values of b/t than 2.5. This indicates that the mobilized passive stress in the geocell pocket size under lateral displacement increase to an optimum value. But when, the pocket size value is higher than the optimum one, the contribution of these passive decreases and it can be seen that the slope stability improvement has been decreased. These results are related to geocell confinement mechanism. Each geocell pocket confines in filled materials and as the geocell pocket size increases, this confinement was increased until it reaches an optimum value. Upon reaching the optimum value, an increase in geocell pocket size causes to reduce the area affected by geocell confinement mechanism. This reduction leaded to estimated lower safety factor and higher slope displacement.

To determine the effect of geocell thickness, depth of first layer, vertical spacing and relative density were considered constant (2 m, 2 m and 60%) and the thickness (t) was non-dimensioned versus slope height. The obtained IF values for different thicknesses are shown in Fig. 11. This graph shows that the safety factor increases by increasing the geocell thickness due to the increase in the passive resistance mobilized in front of each geocell strip. This passive resistance is one of the geocell confinement components. However, for $t/H_t > 0.025$ the rate of safety factor improvement has been decreases and does not have significant influence. This can show that the geocell stiffness was increased by increasing the thickness. This caused to geocell deformed harder and the rate of mobilized passive stresses was decreased. Therefore, it can be concluded that the ideal geocell thickness is 1.5%-2.5% of the slope height.

Table 3 gives IF factor and the maximum horizontal displacement of the slope (u_{max}) for different soil relative densities. This table demonstrates that the increase in soil relative density leads to decrease in the maximum lateral displacement and consequently increase in safety factor of slope stability by about 10%. This behavior is related to the soil particle better interlocking. Also, this Table 3 gives the obtained maximum induced geocell membrane stress that induced in the geocell pocket perimeter for different soil

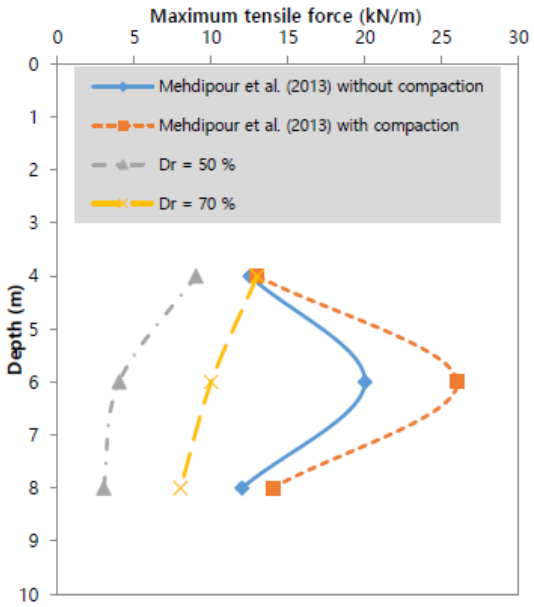

Fig. 12 Comparison between obtained and Mehdipour *et al*. (2013) maximum tensile force in geocell layer

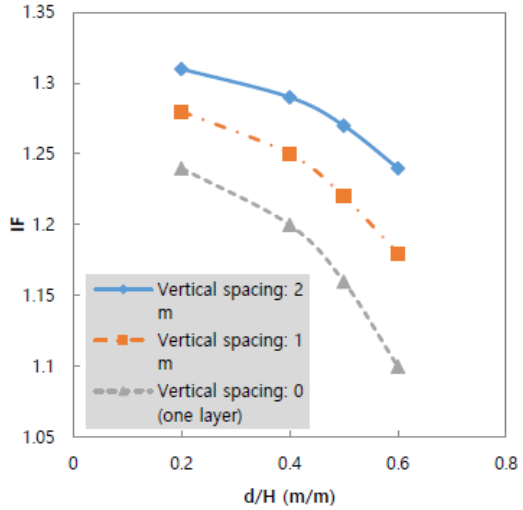

Fig. 13 Variation of IF factor versus depth of first geocell layer

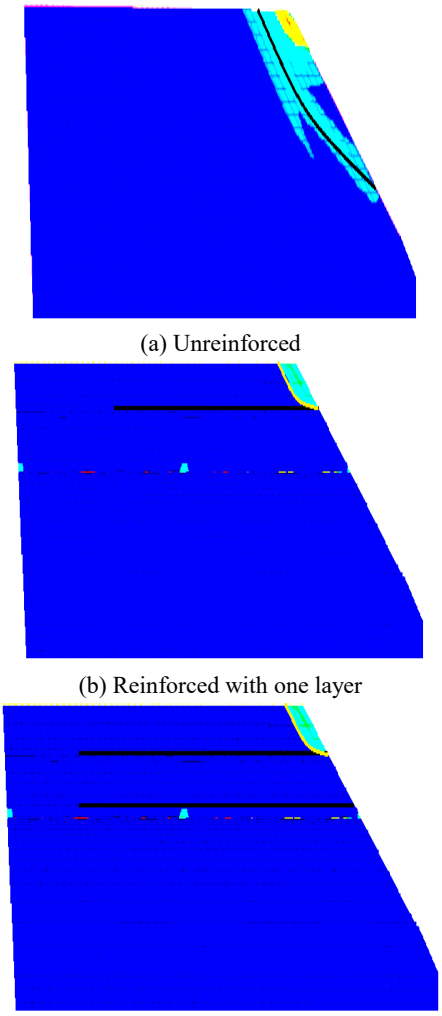

(a) Unreinforced

(b) Reinforced with one layer

(c) Reinforced with two layers

Fig. 14 Induced slip surface

relative densities. It is obvious that for higher soil relative densities, the mobilized stress in geocell has been increased due to the higher confinement stress and soil passive pressure.

Mehdipour *et al*. (2013) investigated this behavior by simulating compaction process but they used equivalent two dimensional analyses and did not consider the elastoplastic behavior of geocell. Fig. 15 compares the obtained maximum tensile force in the geocell layer after and before compaction by Mehdipour *et al*. (2013) with the loose and dense condition of simulated three dimensional slope. In order to carry out this comparison, three geocell layers used in 4, 6 and 8 m depth from top of the slope crest. The length of these layers was kept constant and equal to 20 m. Moreover, the geocell thickness, aperture size and secant modulus were set 200 mm, 25 × 25 cm × cm and 150 kN/m, respectively. It can be seen in Fig. 12 that there is huge disagreement between two obtained methods. Simulating the compaction process used by Mehdipour *et al*. (2013) causes to show the maximum tensile force at the second geocell layer. On the other hand, increasing the soil relative density leads to reduce the maximum tensile force by increasing depth. This result indicates that the compaction process simulation does not compact each layer uniformly while relative density method increases the soil density homogeneously. Also, the reason why the maximum tensile force is measured at the first layer, may possibly be the higher displacement occurred at the top of the slope that develops greater tensile force at the shallower geocell mattresses. Furthermore, the difference between the achieved tensile force values in the same layer indicates that the Mehdipour *et al*. (2013) method predicts higher tensile force. This can be related to elastoplastic behavior of geocells which has not be considered in the two dimensional equivalent model.

Fig. 13 presents the IF factor versus depth of first geocell layer (d) for different vertical spacing. In this graph, the depth of first geocell layer is non-dimensioned versus slope height. The evaluation of this figure shows that the increase in first geocell layer leads to decrease in IF factor.

The rate of this decrease is reduced for first geocell layer placement lower than 0.5H. Furthermore, it can be seen that the increase in vertical spacing of geocell layers will increase the rate of slope stabilization especially for $d/H >$ 0.4. This shows that the placement of geocell layers affect the slip surface. Fig. 14 illustrates the slip surface for unreinforced, one layer reinforced and two layers reinforced slope. The induced slip surface indicates that the critical failure surface is highly depended to the first geocell layer placement and it is limited to the upper part of first geocell layer. However, it can be seen that the second geocell layer placement does not have any significant influence on the slip surface. It can be inferred that first geocell strip restrain the slip surface from developing to the lower layers.

5. Conclusions

In the present research, a series of full three-dimensional geocells were modeled in order to investigate the effect of geocell on the slope stability. The geocell and soil were simulated separately in 3D using finite difference method. In these analyses the effects of aperture size, thickness, soil compaction, suitable geocell layer placement and vertical spacing between geocell mattresses were investigated. Hence, the subsequent conclusions were drawn:

• It was found that the slope stability first increases and then decreases as the geocell pocket size increases. This behavior indicated that the contribution of geocell confinement components: passive stress occurred in the cells is depended on the geocell pocket size and after a specific value, this contribution decreased. Hence, the maximum slope stability and minimum lateral displacement in the condition of this study took place when $b/t = 2.5$.

• Geocell thickness has significant influence on the safety factor. The slope factor of safety increases by increasing geocell thickness but the rate of increase in slope stability decreases during an increase of thickness and it does not have significant effect for $t/H_t > 0.025$. Therefore, the optimum geocell thickness range is 1.5%-2.5% of the slope height.

• The results showed that increasing soil relative density and consequently compaction leaded to increase slope safety factor and decrease maximum lateral displacement. This effect is related the higher confinement stress and soil passive pressure which increase the induced membrane stresses along geocell pocket elements.

• By placing first geocell layer in lower depth, the IF value increases and it restrains the critical failure surface. Also, it was concluded that using two geocell layers with higher vertical spacing leads to reduce the failure potential. However, the second geocell layer does not have any significant effect on the critical failure surface due to the high stiffness of first geocell mattress.

References

Ardakani, A., Bayat, M. and Javanmard, M. (2014), "Numerical modeling of soil nail walls considering Mohr Coulomb, hardening soil and hardening soil with small-strain stiffness effect models", *Geomech. Eng.*, **6**(4), 391-401. http://dx.doi.org/10.12989/gae.2014.6.4.391.

Arvin, M., Zakeri, A. and Shoorijeh, M.B. (2019), "Using finite element strength reduction method for stability analysis of geocell-reinforced slopes", *Geotech. Geol. Eng.*, **37**(3), 1453-1467. https://doi.org/10.1007/s10706-018-0699-0.

Bayat, M., Bayat, M. and Pakar, I. (2018), "Nonlinear vibration of oscillatory systems using semi-analytical approach", *Struct. Eng. Mech.*, **65**(4), 409-413. http://doi.org/10.12989/sem.2018.65.4.409.

Bayat, M., Pakar, I. and Bayat, M. (2016), "Nonlinear vibration of rested Euler-Bernoulli beams on linear elastic foundation using Hamiltonian approach", *Vibroeng. Proc.*, **10**, 89-94.

Biswas, S. and Mittal, S. (2017), "Square footing on geocell reinforced cohesionless soils", *Geomech. Eng.*, **13**(4), 641-651. http://dx.doi.org/10.12989/gae.2017.13.4.641.

Chen, R.H. and Chiu, Y.M. (2008), "Model tests of geocell retaining structures", *Geotext. Geomembr.*, **26**, 56-70. https://doi.org/10.1016/j.geotexmem.2007.03.001.

Chen, R.H., Huang, Y.W. and Huang, F.C. (2013), "Confinement effect of geocells on sand samples under triaxial compression", *Geotext. Geomembr.*, **37**, 35-44. https://doi.org/10.1016/j.geotexmem.2013.01.004.

Dai, Z., Zhang, M., Yang, L. and Zhu, H. (2018), "Model tests on performance of embankment reinforced with geocell under static and cyclic loading", *Proceedings of GeoShanghai International Conference: Ground Improvement and Geosynthetics*, Shanghai, China, May.

Dash, S.K. (2010), "Influence of relative density of soil on performance of geocell reinforced sand foundations", *J. Mater. Civ. Eng.*, **22**(5), 533-538. https://doi.org/10.1061/(ASCE)MT.1943-5533.0000040.

Dash, S.K. (2012), ''Effect of geocell type on load carrying of geocell reinforced sand foundations", *Int. J. Geomech.*, **12**(5), 537-548. https://doi.org/10.1061/(ASCE)GM.1943-5622.0000162.

Dash, S.K., Krishnaswamy, N.R. and Rajagopal, K. (2001), "Bearing capacity of strip footings supported on geocell-reinforced sand", *Geotext. Geomembr.*, **19**(4), 235-256. https://doi.org/10.1016/S0266-1144(01)00006-1.

Dash, S.K., Sireesh, S. and Sitharam, T.G. (2003), "Model studies on circular footing supported on geocell reinforced sand underlain by soft clay", *Geotext. Geomembr.*, **21**(4), 197-219. https://doi.org/10.1016/S0266-1144(03)00017-7.

Garcia, R.S. and Neto, J.A. (2021), "Stress-dependent method for calculating the modulus improvement factor in geocell-reinforced soil layers", *Geotext. Geomembr.*, **49**(1), 146-158. https://doi.org/10.1016/j.geotexmem.2020.09.009.

Guerrero, S.L. and Vallejo, L.E. (2010), "The effectiveness of Geosynthetic reinforcement, tamping, and stoneblowing of rail track ballast beds under dynamic loading: DEM analysis", *Geomech. Eng.*, **2**(3), 161-176. http://doi.org/10.12989/gae.2010.2.3.161.

Guo, W., Chu, J., Yan, S. and Nie, W. (2014), "Analytical solutions for Geosynthetic tube resting on rigid foundation", *Geomech. Eng.*, **6**(1), 65-77. http://doi.org/10.12989/gae.2014.6.1.065.

Halder, K. and Chakrabotry, D. (2020), "Influence of soil spatial variability on the response of strip footing on geocell reinforced slope", *Comput. Geotech.*, **122**, 103533. http://doi.org/10.1016/j.compgeo.2020.103533.

Hedge, A. and Sitharam, T.G. (2016), "Behaviour of geocell reinforced soft clay bed subjected to incremental cyclic loading", *Geomech. Eng.*, **10**(4), 405-422. http://doi.org/10.12989/gae.2016.10.4.405.

Itasca (2005), *Fast Lagrangian Analysis of Continua in 3 Dimensions User's Manual*, Itasca Consulting Group, Minnesota, U.S.A.

Jesmani, M., Kamalzare, M. and Sarbandi, B.B. (2016), "Seismic response of geosynthetic reinforced retaining walls", *Geomech. Eng.*, **10**(5), 635-655. http://dx.doi.org/10.12989/gae.2016.10.5.635.

Kazemian, T. and Arvin, M.R. (2019), "Three-dimensional stability of locally loaded geocell-reinforced slopes by strength reduction method", *Geomech. Eng.*, **14**(3), 185-201. https://doi.org/10.1080/17486025.2019.1581275.

Khalaj, O., Tafreshi, S.N.M., Masek, B. and Dawson, A.R. (2015), "Improvement of pavement foundation response with multi layers of geocell reinforcement: Cyclic plate load test", *Geomech. Eng.*, **9**(3), 373-395. http://doi.org/10.12989/gae.2015.9.3.373.

Krishnaswamy, N.R., Rajagopal, K. and Latha, G. (2000), "Model studies on geocell supported embankments constructed over a soft clay foundation", *Geotech. Test. J.*, **23**, 45-54. https://doi.org/10.1520/GTJ11122J.

Kumar, A., Singh, P. and Chatterjee, K. (2019), "Ground improvement using geocells to enhance traffic ability in desert soils", *Geomech. Eng.*, **19**(1), 71-78. https://doi.org/10.12989/gae.2019.19.1.071.

Latha, G.M. (2011), "Design of geocell reinforcement for supporting embankments on soft ground", *Geomech. Eng.*, **3**(2), 117-139. http://dx.doi.org/10.12989/gae.2011.3.2.117.

Latha, G.M. and Rajagopal, K. (2007), "Parametric finite element analyses of geocell supported embankments", *Can. Geotech. J.*, **44**(8), 917-927. https://doi.org/10.1139/T07-039.

Latha, G.M. and Somwanshi, A. (2009), "Effect of reinforcement form on the bearing capacity of square footings on sand", *Geotext. Geomembr.*, **27**(6), 409-422. https://doi.org/10.1016/j.geotexmem.2009.03.005.

Latha, L.G., Dash, S.K. and Rajagopal, K. (2008), "Equivalent continuum simulations of geocell reinforced sand beds supporting strip footings", *Geotech. Geol. Eng.*, **26**, 387-398. https://doi.org/10.1007/s10706-008-9176-5.

Leshchinsky, B. and Ling, H.I. (2013), "Effects of geocell confinement on strength and deformation behavior of gravel", *J. Geotech. Geoenviron. Eng.*, **139**(2), 340-352. https://doi.org/10.1061/(ASCE)GT.1943-5606.0000757.

Ling, H.I., Leshchinsky, D., Wang, J.P., Mohri, Y. and Rosen, A. (2009), "Seismic response of geocell retaining walls: Experimental studies", *J. Geotech. Geoenviron. Eng.*, **135**(4), 515-524. https://doi.org/10.1061/(ASCE)1090-0241(2009)135:4(515).

Mehdipour, I., Ghazavi, M. and Moayed, R.Z. (2013), "Numerical study on stability analysis of geocell reinforced slopes by considering the bending effect", *Geotext. Geomembr.*, **37**, 23-34. https://doi.org/10.1016/j.geotexmem.2013.01.001.

Mehdipour, I., Ghazavi, M. and Moayed, R.Z. (2017), "Stability analysis of geocell reinforced slopes using the limit equilibrium horizontal slice method", *Int. J. Geomech.*, **17**(9), 1-15. https://doi.org/10.1061/(ASCE)GM.1943-5622.0000935.

Moltagh, A.T., Ghanbari, A., Abbasi, P.M. and Wu, W. (2018), "A new analytical approach to estimate the seismic tensile force of geosynthetic reinforcement respect to the uniform surcharge of slopes", *Earthq. Struct.*, **15**(6), 687-699. http://dx.doi.org/10.12989/eas.2018.15.6.687.

Oliaei, M. and Kouzegran, S. (2017), "Efficiency of cellular geosynthetics for foundation reinforcement", *Geotext. Geomembr.*, **45**(2), 11-22. https://doi.org/10.1016/j.geotexmem.2016.11.001.

Ou, C.Y. (2006), *Deep Excavation: Theory and Practice*, CRC Press, London, U.K.

Saride, S., Pradhan, S., Sitharam, T.G. and Puppala, A.J. (2013), "Numerical analysis of geocell reinforced ballast overlying soft clay subgrade", *Geomech. Eng.*, **5**(3), 263-281. http://doi.org/10.12989/gae.2013.5.3.263.

Shimizu, M. and Inui, T. (1990), *Increase in the Bearing Capacity of Ground with Geotextile Wall Frame*, Balkema, Rotterdam, Netherlands.

Song, F. and Tian, Y.H. (2019), "Three-dimensional numerical modelling of geocell reinforced soils and its practical application", *Geomech. Eng.*, **17**(1),1-9. https://doi.org/10.12989/gae.2019.17.1.001.

Song, F., Liu, H.B., Chai, H.B. and Chen, J.X. (2017), "Stability analysis of geocell reinforced retaining walls", *Geosynth. Int.*, **24**(5), 442-450. https://doi.org/10.1680/jgein.17.00013.

Song, F., Liu, H., Ma, L. and Hu, H. (2018), "Numerical analysis of geocell-reinforced retaining wall failure modes", *Geotect. Geomembr.*, **46**(18), 284-296. https://doi.org/10.1016/j.geotexmem.2018.01.004.

Tafreshi, S.M., Shaghaghi, T., Mehrjardi, G.T., Dawson, A.R. and Ghadrdan, M. (2015), "A simplified method for predicting the settlement of circular footings on multi-layered geocell-reinforced noncohesive soils", *Geotext. Geomembr.*, **43**(4), 332-344. https://doi.org/10.1016/j.geotexmem.2015.04.006.

Tavakoli, G.H.M., Tafreshi, S.N.M. and Dawson, A.R. (2013), "Combined use of geocell reinforcement and rubber-soil mixtures to improve performance of buried pipes", *Geotext. Geomembr.*, **34**, 116-130. https://doi.org/10.1016/j.geotexmem.2012.05.004.

Won, M.S., Lee, O., Kim, Y.S. and Choi, S. (2016), "An 12 year long term study on the external deformation behavior of Geosynthetic reinforced soil (GRS) walls", *Geomech. Eng.*, **10**(5), 565-575. http://doi.org/10.12989/gae.2016.10.5.565.

Zhao, M. and Zhao, H. (2013), "Deformation analysis of a Geocell mattress using a decoupled iterative method", *Struct. Eng. Mech.*, **46**(6), 775-790. http://dx.doi.org/10.12989/sem.2013.46.6.775.

Zhao, M.H., Zhang, L., Zou, X.J. and Zhao, H. (2009), "Research progress in two-direction composite foundation formed by geocell reinforced mattress and gravel piles", *Chin. J. Highway Transport*, **22**(1), 1-10.

GC